IEEE Access
Multidisciplinary | Rapid Review | Open Access Journal

Received 26 April 2024, accepted 21 July 2024, date of publication 29 July 2024, date of current version 7 August 2024.

Digital Object Identifier 10.1109/ACCESS.2024.3434681

RESEARCH ARTICLE

Exploring Quantum Machine Learning for Enhanced Skin Lesion Classification: A Comparative Study of Implementation Methods

S. SOFANA REKA[1], H. LEELA KARTHIKEYAN[2], A. JACK SHAKIL[2], PRAKASH VENUGOPAL[2], AND MANIGANDAN MUNIRAJ[2]

[1]Centre for Smart Grid Technologies, School of Electronics Engineering, Vellore Institute of Technology, Chennai 600127, India
[2]School of Electronics Engineering, Vellore Institute of Technology, Chennai 600127, India

Corresponding author: Prakash Venugopal (Prakash.v@vit.ac.in)

This work was supported by the Vellore Institute of Technology, Chennai.

ABSTRACT Skin diseases affect millions of people worldwide, leading to significant healthcare burdens and challenges in diagnosis and treatment. In the past few years, machine learning techniques have demonstrated potential in assisting dermatologists with diagnosing various skin conditions. As in, conventional machine learning algorithms might encounter challenges in handling the complexity and distinction of skin disease classification tasks, primarily because of the intricate nature of medical image data with its high dimensional properties. In this work, the main analysis is done based on exploring quantum machine learning models for skin disease classification. This approach blends with the aspects of quantum computing with the conventional machine learning techniques to push the boundaries of skin disease classification. This work harnesses the HAM10000 dataset, an extensive compilation of categorized images portraying common skin lesions, to train and assess the efficacy of the proposed methodologies. Quantum computing libraries such as PennyLane and Qiskit is used in this study. Using different combination of qubit rotation encoding and decoding using three types of Pauli gates such as Pauli X, Y and Z gates are implemented and compared using proposed Quanvolutional neural network. Features extracted using MobileNet pre-trained network is used to build Quantum support vector classifier. These quantum machine learning models are compared with some well-known pre-trained models such as Resnet50, Inception-Resnet, Densenet121, DenseNet201 and MobileNet. The combination of RY qubit rotation and PauliZ gate in quantum convolution layer in Quanvolutional neural network produced the optimal classification accuracy of 82.86% more than any other models included in this study. In contrast, Quantum Support Vector Classifier produced similar classification accuracy of 72.5% with respect to pre-trained models.

INDEX TERMS HAM10000 dataset, Qiskit, quantum machine learning, quanvolutional neural network, quantum support vector classifier, skin lesion, PennyLane.

I. INTRODUCTION

An estimated 1.8 billion people worldwide suffer from skin-related conditions at any given moment. Skin cancer remains the most prevalent cancer globally, with an alarmingly rising incidence rate. Skin infections, stemming from microbial, viral, fungal, or parasitic induced roots are the prevailing disease contributors in tropical and settings with limited resources. Within most societies, skin-related neglected tropical diseases (skin NTDs) account for close to one-tenth

The associate editor coordinating the review of this manuscript and approving it for publication was Valentina E. Balas.

of all skin diseases. As a result, it is crucial for ailing countries to embrace a comprehensive and people-based approach for managing skin NTDs and various skin conditions within the scope of universal health coverage. The World Health Organization acknowledges about twenty diseases and groups of diseases as neglected tropical diseases. It is important to use beneficial strategies to enhance the control of diseases and healthcare through sharing resources and opportunities, as advised by WHO. When it comes to these diseases, approximately 9 consist of skin issues. Unlike diseases that can be handled through mass drug administration (MDA), where entire populations in specific areas are treated, some skin NTDs need personalized diagnosis and treatment. In general, these treatments require a sustained level of commitment and significant resources. The provision of sufficient care to the affected individuals becomes highly complicated due to the limited healthcare infrastructure and poorly trained personnel in those remote areas, where skin NTDs are quite prevalent. Therefore, it is of utmost critical importance to address the challenges faced in treating skin NTDs in a holistic manner for better healthcare outcomes [1].

In 2017 study, the understanding towards adjusted life years disability for fungal skin diseases (DALY) varied with age, showing a peak between 1 and 5 years. Sub-Saharan Africa bore the heaviest burden, with a DALY rate of 89.3 per 100,000 males and 78.42 for females. Mali had the highest DALY rate at 122. On the other hand, areas characterized by affluent economies, such as southern Latin America, western Europe, Australasia, North America, and southern Pacific regions, exhibits the lowest burden recording a DALY rate of 33.12 per 100,000 males and 30.16 for females. In conclusion, fungal skin diseases significantly impact patients worldwide, especially in resource-poor countries, tropical regions, and among children aged 1 to 5 years. Using DALYs as a metric could guide health policies to mitigate greater impact on fungal based skin diseases [2]. Skin cancer is a big health issue in India, a country with lots of people from different backgrounds. Studies show that the number of skin diseases, including ones that might be cancer, is going up. It ranges from about 7.9% to 60% in different parts of the country. This wide range is influenced by things like how much money people have and how easy it is to get healthcare. According to a 2017 study, skin diseases comprised 4.02% of the overall disability-adjusted life years (DALYs) in India. Skin based diseases have become more common in recent years, putting a strain on healthcare systems worldwide. In India, the duration of time individuals spent living with disabilities because of malignant melanoma increased a lot between 1990 and 2017, by 215.7%. Additionally, squamous cell carcinoma and basal cell carcinoma among other skin cancer types experience considerable rises, with growth rates of 96.8% and 90.9% respectively. But most of the information we have about skin diseases in India comes from small studies or surveys done in hospitals or communities, so we may not know the full extent of the problem [3].

The skin is our body's largest organ which serves as a crucial barrier against infections. It protects internal organs, regulates body temperature, and allows us to feel touch. Skin has three main layers such as epidermis, dermis, and hypodermis where each layer performs distinct functions. Additionally, the skin shields us from harmful UV radiation, with melanin determining our skin color. Given its vital role in safeguarding the body, prioritizing skincare is essential. Untreated skin conditions can spread to other body parts, causing serious issues, especially considering the contagious nature of some diseases. Among skin diseases, skin cancer poses the greatest threat. Non-communicable diseases (NCDs) contribute to a significant percentage of global and Indian mortality rates [4]. Cancer is one of the deadliest diseases. Of all the cancers, skin cancer has the fastest chance of being cured if detected early. It is progressively vital aspect of common health, with rapidly expanding practice. The three different definitions of skin cancer are Squamous Cell Carcinoma (SCC), Basal Cell Carcinoma (BCC) and Melanoma. Non-melanoma skin cancer emerges as the most common and dangerous, causing approximately one million cases annually and bringing in 64,000 cases each other in the world. In particular, the incidence of non-melanoma skin cancer shows a significant gender difference, with men suffering approximately twice as much as women. The burden of this malignancy is higher in Australia and New Zealand where it is more likely to develop cancer [5]. This one is the preeminent deadly kind of cancer because it spreads its roots to other body parts and penetrates the skin more deeply if it is not detected too soon. It is impossible to overstate the importance of detecting melanoma early in its modification. Because of this, early detection could potentially save numerous lives. Thus, it is imperative to take seriously any suspicious lesion that manifests anywhere on the skin. Early identification of malignant melanoma is paramount [6].

Early and accurate diagnosis is paramount for successful treatment and improved patient outcomes. Automated skin lesion cancer classification using image analysis techniques has emerged as a promising avenue in this domain. Machine learning and deep learning algorithms in this analysis of skin diseases has exhibited good performances in examining skin lesion images and finding differences between benign and malignant lesions. A proposed approach outlines a hair removal system digitally that utilizes filtering based on morphological techniques including different algorithms like black hat and in painting based algorithms with an automatic Grab cut segmentation technique for lesion detection employing two process of clustering aspects with K means method and also involving hue based saturation value with color space parameter [7]. After extracting features from the Gray Level Co-occurrence Matrix and statistical parameters followed by the three machine learning classification systems considering K nearest algorithm (KNN), support vector machine modelling (SVM) and decision tree algorithm in which SVM resulted in 97% accuracy. Incorporating Fuzzy

clustering combined with features aspect of both involving KNN and also SVM based classification techniques utilizing analysis based on wavelet is used for 50 samples, revealing KNN's better accuracy of 91.2% compared to SVM [8].

The past few years have exhibited a significant aspect on deep learning models for the detection and categorization of skin cancer. This part offers a synopsis of key literature to the advancement of this area. A hybrid and deep convolutional network known as Inception ResNet V2 for classifying skin cancer images was proposed [9]. The main aspect of this work is to examine the efficacy of the specified model by performing enhancement on the dataset by augmenting images using affine transformation techniques which increases the volume of available data for training. Therefore, the augmented showed a notable improvement obtaining an accuracy of 95.09% while the original dataset only managed to reach an accuracy of 83.59%. This work exhibits on categorizing different types of skin cancers which are analyzed based on Mobile Net CNN with pre trained modelling. After removing the final five layers, a new dense layer featuring SoftMax activation was done for predicting the models and a categorical accuracy of 97% was observed [10]. A comparison of models was done based on Adam and SGD optimizers performance. ResNet50 showed the best results among other models and arrived at an accuracy of 90% using SGD optimizer and 88% using Adam optimizer [11]. A DenseNet121 architecture consisting of dropout layers to reduce overfitting and two dense layers with ReLU activation to capture nonlinear interactions and a SoftMax activation function is utilized by the output layer for effective classification across seven skin disease classes which resulted in 95.75% accuracy [12]. DenseNet201 with its deeper architecture of 201 layers, has better feature extraction abilities outperformed the other pre-trained models in both plain and hierarchical classifiers with two levels. The initial phase focused on distinguishing nevi from non-nevi images, whereas the following level classified malignant moles among non-nevi cases. An experiment conducted to classify nevi from non-nevi images, and malignant moles among non-nevi cases. Results showed that DenseNet201 achieved about 10% better than other deep networks on all metrics [13]. Xception-ResNet50 (X-R50) model is proposed to classify different types of skin cancer in HAM10000 dataset. The proposed concatenated X-R50 achieved a 97.8% prediction accuracy [14]. A merged model of ResNet-50, and VGG-16 is proposed for classifying skin lesions. The accuracy achieved by the proposed system is up to 94.14% [15].

The theory of Moore's law, suggesting a doubling in the number of transistors on a microchip every two years, has been the reason behind computer technology progress for decades, but as transistors shrink and approach physical limits, maintaining this number will become more challenging. As transistors edge closer to the atomic scale and production costs climb, the traditional technological impetus propelling Moore's Law in fifty years is collapsing and is expected to level out by 2025. Many experts say that we are approaching the practical limits of Moore's Law in terms of traditional silicon-based computing [16]. Quantum computing gives a potential answer to this problem by making use of quantum mechanics principles to execute calculations in fundamentally different methods than classical computers. The quantum bit, also referred as qubit, serves as the essential unit in quantum computing, and it can occupy multiple states at the same time based on different phenomena like superposition properties and entanglement. This enables quantum computers to do certain sorts of calculations significantly more efficiently than traditional computers [17]. One key advantage of quantum computing over classical computing is its potential to solve certain types of problems much faster. For example, quantum computers have shown promise in solving optimization problems, factoring large numbers, and simulating quantum systems. Within machine learning, QML harnesses quantum computing techniques by improving the performance and efficacy of different learning algorithms. QML algorithms supports various unique properties of qubits to perform tasks such as data classification, clustering, and regression more efficiently than classical machine learning algorithms in certain scenarios. Some ways in which quantum computing can enhance machine learning by faster training time, improved feature mapping, enhanced optimization and quantum pre-processing [18]. Today, intelligent technologies such as pattern recognition, data mining, and deep learning proficiently address the challenges associated with medical images, liberating craftsmanship, improving accuracy, and greatly improves accuracy and performance but their programs tend to be complex and time intensive. Quantum Machine Learning (QML) brings the leverage of speed and model refinement, offering potential solutions for the challenges. Making use of the remarkable data processing capabilities of classical computers, researchers influenced by quantum mechanics have explored a variety of quantum computing models to tackle n-dimensional objects as well as data high-quality aspects of clinical images that can be suitable for study using QML [19]. Most real-world data reside in classical computers. Seamless integration between classical and quantum systems for data processing and training QML models is a significant challenge.

Quantum transfer learning applies a classical VGG16 layer with a multiqubit QML layer on Eurosat and synthetic datasets, and an UC Merced Land use dataset which has high dimensional data and challenging classification objectives [20]. The MNIST and Fashion MNIST datasets served as the backdrop for introducing a quantum neural network model which is influenced by CNN relied only on two qubit interrelations in the whole algorithm. Referred to as Quantum Convolutional Neural Network (QCNN), it demonstrated superior classification accuracy compared to the CNN model, despite featuring fewer free parameters [21]. Using the Eurostat dataset as the reference benchmark, a novel QCNN technique is tested for the geographic analysis which

is selected as an Earth observation (EO) use case. The suggested model achieved a 98% overall F1 score and 98% overall accuracy [22]. The Pegasos Quantum Support Vector Classifier (QSVC) was proposed for multi-class cardiovascular disease classification. The results indicated that the QSVC performed significantly better than the traditional Support Vector Classifier (SVC), showcasing gains of +9.72% and +10.76%, respectively, in comparison to both the QSVC as well as the Pegasos QSVC. The research also investigated a quantum deep learning methodology with an implementation of special Quanvolutional Neural Network (QNN). Demonstrating remarkable performance, this model achieved an accuracy, precision, recall, F1 score, and specificity of 97.31%, 97.41%, 97.31%, 97.30%, and 99.10% respectively. It is noteworthy that it performed an extra +3.88% better than its classical Convolutional Neural Network (CNN) equivalent and all other models combined [23]. In a study, the Cleveland heart disease data collection, featuring two classes denoting disease presence or absence, served as the basis for comparing the Quantum support vector classifier (QSVC) against the classical support vector classifier (SVC). QSVC outperformed classical SVC with the accuracy of 88.52% and 85.24% respectively [24]. Support vector classifier (SVC) algorithm outperformed the other algorithms such as QSVC, XG-Boost and Variational quantum classifier (VQC) with the accuracy of 95.08%. The training time of quantum algorithm-based models is relatively high than classical models [25]. Two quantum classifiers, namely quantum support vector classifiers (QSVC) and variational quantum classifiers (VQC), were examined to assess their performance in predicting chronic heart disease within the healthcare 4.0 ecosystem. QSVC's success rate was better than VQC with an accuracy of 82% [26]. An ensemble machine learning strategy, incorporating quantum classifiers, is proposed for accurate prediction of heart disease risk. The suggested approach adopts a bagging ensemble approach, with a quantum support vector classifier acting as the primary classifier. The Bagging QSVC model produced 90.16% of classification accuracy which outperforms all other models [27]. The CH, HOG, and features extracted by auto encoder were classified utilizing classical SVM and quantum SVM techniques on the PH2 dataset. On several instances, it has been evident that the classical method has consistently shown excellence over the quantum-based technique [28]. Despite the considerable potential of quantum computing in redefining fields such as machine learning, it is essential to recognize that practical quantum computers remain in the budding phases of development. Significant technical challenges remain to be addressed, such as improving qubit coherence and reducing error rates, before quantum computing can realize its full potential. Nonetheless, research in this area continues to progress rapidly, and quantum machine learning remains an exciting area of exploration for the future of computing. The following points were observed from the literature study:

- Pre-trained networks such as Resnet50, Densenet121, Densenet201, Inception-Resnet and MobileNet produced satisfying results on datasets based on skin diseases.
- Quantum machine learning algorithms are in its nascent stages.
- Benchmark quantum machine learning algorithms such as variational quantum classifiers (VQC), Quantum Convolutional neural network (QCNN) and quantum support vector classifier (QSVC) have been used recently across different research domains.
- Only few researchers have analyzed the impact of quantum machine learning models in exploring skin diseases.
- Many researchers have performed binary classification using QML algorithms.

Based on the findings, an innovative novel comparative approach is introduced for diagnosing skin lesion classification in alignment with the stated motivations.

- A multi-classification approach is proposed using quantum machine learning for classifying skin lesions.
- Quantum machine learning models such as Quanvolutional neural network and quantum support vector classifier (QSVC) are implemented.
- Various quantum encoding and decoding methods have been implemented in Quanvolutional neural network and analyzed.
- This research conducts a comparative study to assess the performance and impact of classical models versus quantum models.

II. MATERIALS AND METHODS

A. HAM10000 SKIN LESIONS DATASET

In this study, we have used the (''Human Against Machine with 10000 training images'') HAM10000 dataset which consists of 10015 dermatological images, this dataset is openly accessible through ISIC archive, providing a valuable resource for intellectual machine learning purposes. This dataset serves as a benchmark for machine learning as well as evaluations with human experts. Cases are drawn from a wide range of important medical categories in the domain of skin lesions. A significant majority of the lesions have histopathological confirmation, whereas the remaining cases are proven by subsequent inspection, consensus among specialists, verification via in-vivo confocal microscopy [29]. The dataset description is shown below in Table 1. Fig. 1 exhibits different types of skin cancer and its samples.

B. DATA AUGMENTATION AND DATA PROCESSING

In this analysis data augmentation includes different range of methods including both the size and the quality of the datasets based on enabling the design aspects with the deep learning models. Numerous image-based augmentation process which includes transformation based on geometric analysis, adjustments which is involved with the color space and also with different kernel filters and also involves various image

TABLE 1. Dataset description.

Skin Lesion Type	Label	Description	Size
Melanocytic nevi	nv	Commonly known as moles, are benign (non-cancerous) growths on the skin that develop when melanocytes (cells that produce pigment) grow in clusters [31].	6705
Melanoma	mel	Arises from melanocytes, the cells responsible for skin pigmentation. It can occur anywhere on the body. Melanomas may have a larger diameter than normal moles [32].	1113
Benign keratosis-like lesion	bkl	Also known as seborrheic keratoses, are non-cancerous growths that commonly appear on the skin, especially in older individuals [33].	1099
basal cell carcinoma	bcc	Most prevalent skin cancer type, typically appearing on sunlight exposed body regions such as the face, neck, and arms [34].	514
Actinic keratoses/ Bowen's disease	akiec	Generally considered precancerous, they can progress to squamous cell carcinoma if left untreated. It develops on areas of the skin that have been exposed to ultraviolet (UV) radiation from the sun [35].	327
vascular	vasc	Abnormalities in the blood vessels of the skin, which can manifest in various forms [36].	142
dermatofibroma	df	These are benign (non-cancerous) skin growths that typically appear as firm, raised nodules on the skin. They are commonly found on the legs, although they can occur on any part of the body[37].	115

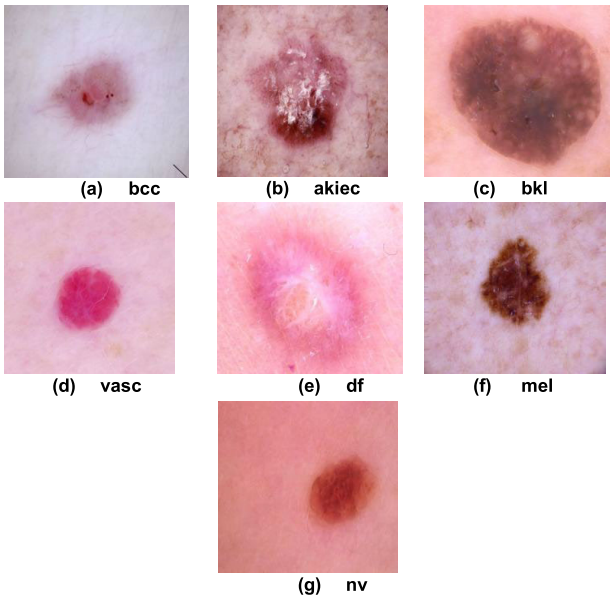

FIGURE 1. Images (a) to (g) are seven skin lesions in HAM10000 dataset.

mixing. This also includes random erasing, augmentation of feature space, generative adversarial networks, adversarial training, meta learning process, transfer based on neural networks which have been employed in numerous research studies. Overfitting occurs when a network learns a function with excessive variance, resulting in an overly precise representation of the training data. Unfortunately, not all application domains like medical image analysis have access to big data [30]. In this study, a dataset comprises 10,015 images across 7 classes, initially imbalanced. Some normal data augmentation methods such as rotations, flipping, enhancing contrast and brightness and noise tuning have been used randomly on original dataset. This step ensures more equitable representation across classes which enhances the robustness and fairness of subsequent analyses in the research. After augmenting, each class now contains 1,430 images mitigating the class imbalance. Due to the computing resource limitations, 250 random images per class have been considered from 1,430 augmented images. Fig. 2 shows the percentage of different category of data before and after augmentation. Data preprocessing is an important step in deep learning that involves preparing the raw data to make it suitable for training a neural network. It typically involves several operations such as cleaning, transforming, and organizing the data to make sure it is formatted properly that can be effectively utilized by learning algorithms. In this study, common data preprocessing methods such as resizing and normalization are used.

C. RESIZING AND NORMALIZATION

It is a data preprocessing technique commonly used in tasks involving image data, particularly in deep learning applications. It refers to the process of changing the dimensions (height and width) of an image to a desired size to ensure that every image contained in the dataset has consistent dimensions, which is essential for feeding them into the neural network. This helps to improve the computational and memory efficiency, and prevents overfitting. Normalizing in deep learning is the process of scaling input features to a standard range or distribution. It is aimed at grading the scales of all input features, resulting in enhanced integration of training models. In this study, all the pixel values of an image are normalized using a simple normalization method. In image data, pixel values typically range from 0 to 255 representing the intensity of the color channels (red, green, blue). By dividing each pixel value by 255, all of the pixel values are scaled to fall between 0 and 1.

III. PROPOSED METHODOLOGY

In this section, a detailed explanation of the proposed methodology is provided under different sections. Initially, the dataset goes through a data augmentation process which is involved to address different issues for class imbalance. Next,

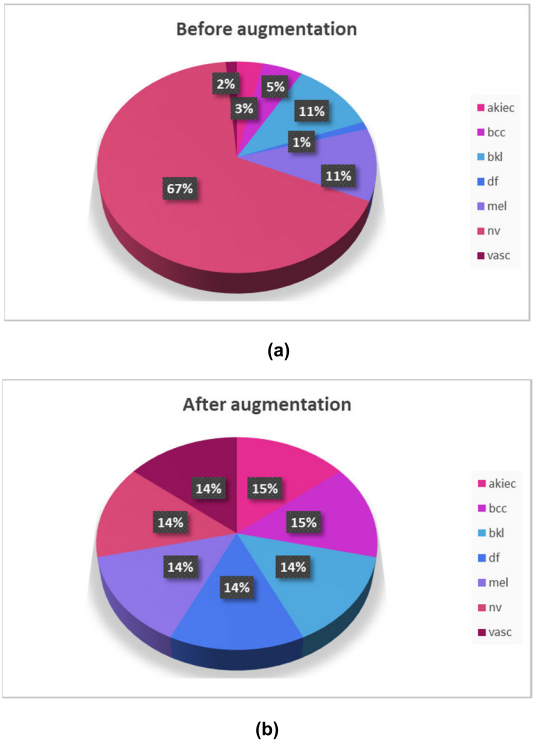

FIGURE 2. Data percentage a) before and b) after data augmentation.

data preprocessing methods are imposed to ensure uniformity across all data. The complete methodology employed in the current study is visually depicted in Fig. 3.

A. PRE-TRAINED DEEP NEURAL NETWORKS (DNN)

Convolutional neural networks (CNNs) are considered to be the subset for deep learning models for better image analysis functions. The strength of CNNs lies in their ability to grasp spatial hierarchies of features within images thereby proving to be effective within tasks such as object classification, image partition and object identification. It typically performs a compilation of sequences, each applying a specific action to the input data. The general architecture of the CNN is shown in Fig. 4. There are different layers associated with CNN,

- The starting layer of the CNN is designated based on the input layer which accepts and also retains the images pixel levels.
- Following the input layer, Convolutional layers are employed. These layers utilize a range of filters on the input data. Each filter is a small matrix of values and the convolutional layer computes its output which is involved in sliding the filter across input data and taking the inner product at each location. Also, it has the ability to learn the edges, corners and objects which are known as hierarchical spatial features in images.
- The pooling layers reduce the spatial resolution of the data. This is done by dividing the data into a grid of cells and then taking the maximum or average value from each cell. Pooling layers assist in decreasing the computational cost of the network and to design the network most robust to noise.
- The next layer is considered to be fully connected layers which plays an important role which involves classification by considering a specified set of values for every set of class which enables activation function to classify in accordance. Fully connected layers identify complicated relationships between features acquired from convolutional layers and pooling layers. Image features are converted from matrix form to vector form using fully connected layers.
- The output generated by the fully connected layers is subsequently used to perform the desired classification, detection, or segmentation tasks.

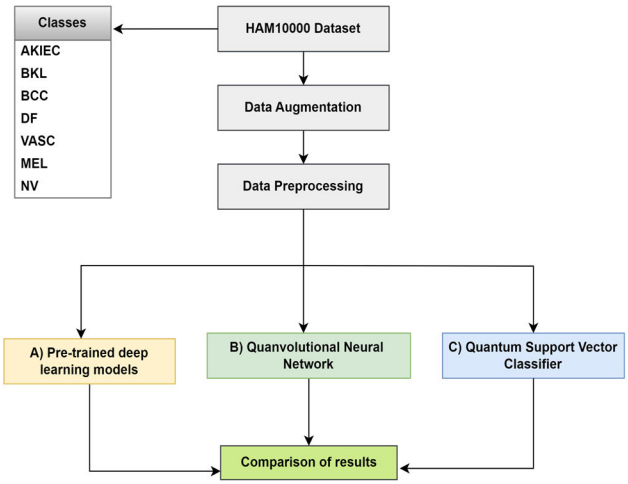

FIGURE 3. Overall proposed methodology.

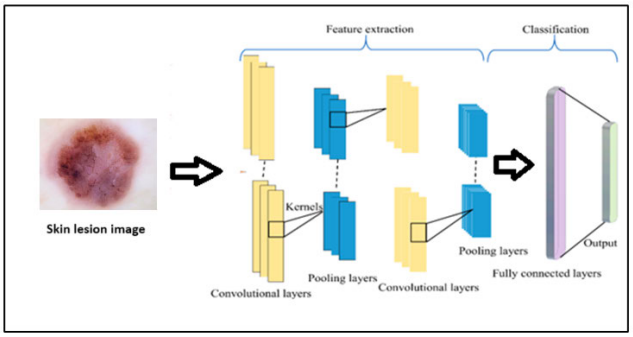

FIGURE 4. General architecture of CNN.

CNNs have been employed across a spectrum of applications such as image classification and segmentation, object detection, medical imaging, and natural language processing. CNNs can learn complex relationships between features in data which makes them very effective at a wide range of applications [38].

B. RESNET50 PRE-TRAINED NETWORK

ResNet50 introduced in 2015 as a pre-trained CNN [39]. ResNet50 came out on top in ImageNet Large Scale Visual.

It follows a technique that allows CNNs to learn deeper and more complex features without overfitting. ResNet architectures are available in many shapes, determined by the quantity of various residual units and the varieties in range of layers starting from 18 to 1202. The effectiveness of the ResNet architecture was enabled by incorporating identity shortcuts wherein the output identity value closely resembled the input values identity. The ResNet architecture shares various similarities with respect to the architecture of VGG. It is notably analysed with the process of eight times very much deeper with respect to VGG which are leading to an increased number of trained features in the architecture. Moreover, the ResNet -50 architecture involved in the process of study exhibits convolutional layers of 49 and also one connected layer in the process.

C. INCEPTIONRESNETV2 PRE- TRAINED NETWORK

InceptionResNetV2 is a deep CNN architecture that combines the Inception and ResNet architectures, to improve feature extraction and classification performance [40]. Developed by Christian Szegedy et al., InceptionResNetV2 was introduced as an extension of the Inception architecture with residual connections, offering a deeper and more efficient network design. The architecture leverages the benefits of both Inception and ResNet models, incorporating multi-level feature extraction from the Inception modules and the residual learning mechanism from ResNet. Through this integration, the network can overcome the vanishing gradient problem that deep networks often encounter while capturing a variety of hierarchical properties. InceptionResNetV2 comprises multiple modules, including Inception modules with varying kernel sizes for feature extraction and residual blocks for facilitating information flow and gradient propagation. The depth and complexity of the architecture enables it to acquire intricate representations from input images, rendering it highly effective for tasks such as image classification and object detection. Additionally, InceptionResNetV2 incorporates auxiliary classifiers and global average pooling layers to improve model robustness and generalization. Trained on extensive image datasets, InceptionResNetV2 demonstrates superior performance in various computer vision applications, with its pre-trained models serving as effective feature extractors or adaptable for fine-tuning on specific tasks.

D. DENSENET201 AND DENSENET121 PRE-TRAINED NETWORK

DenseNet-201 is a deep CNN architecture that has been pre-trained on large image datasets for various computer vision tasks. It is an extension of the original DenseNet architecture (DenseNet-121) and was developed to address challenges in training very deep neural networks while improving accuracy and parameter efficiency. It was introduced in the work Densely Connected Convolutional Networks which has been exhibited [41]. DenseNet201 is a 201-layer CNN that uses a dense connectivity architecture. Dense connectivity is a technique that allows CNNs to learn more complex features by connecting each layer to every other layer. DenseNet201 underwent training on the ImageNet dataset, comprising over 14 million images across 1000 distinct categories. It incorporates a sequence of densely connected convolutional layers within dense blocks, facilitating feature reuse and gradient flow, supplemented by transition layers to manage computational complexity. A global average pooling layer reduces spatial dimensions, succeeded by fully connected layers for classification purposes. DenseNet-201's depth and capacity make it suitable for different concepts of mainly involving classification of images tasks and also detection of objects in varied models with pre-trained models serving as feature extractors or being fine-tuned for specific datasets.

DenseNet-121 is a deep CNN architecture that builds upon the original DenseNet design to address challenges in training deep networks effectively. DenseNet-121 is a 121-layer architecture that makes use of dense connectivity, an important architectural concept that creates dense connections between layers to promote gradient flow and feature reuse. The concept of dense connectedness improves the network's capacity to detect complex patterns and representations, which helps explain why it performs so well across a range of computer vision applications. DenseNet-121 is robust and versatile, making it appropriate for applications like object identification and image classification. Pre-trained models function as efficient feature extractors or can be fine-tuned to specific tasks, making DenseNet-121 a powerful tool in the field of deep learning.

E. MOBILENET PRE-TRAINED NETWORK

MobileNet is a lightweight CNN architecture tailored mainly for efficient mobile and embedded vision applications [42]. The architecture includes several depth wise separable convolutional layers arranged into blocks, with each block followed by a pointwise convolution layer and batch normalization. These blocks serve as the network's backbone and are assigned to extract multi-level features. Additionally, MobileNet contains a global average pooling layer to reduce spatial dimensions and create feature vectors, which are further fed into fully connected layers for classification. With its emphasis on efficiency and compactness, MobileNet strikes a fine blend with model size, computational complexity, and accuracy, making it well-suited for resource limited environments. Pre-trained MobileNet models are widely used as feature extractors in transfer learning applications such as image categorization, object recognition, and semantic segmentation, across diverse range of fields such as computer vision and robotics applications. The Fig. 5 shows the flow diagram of implementation of pre-trained models

F. QUANVOLUTIONAL NEURAL NETWORK - A HYBRID QUANTUM-CLASSICAL MODEL

CNN have swiftly risen to prominence across a spectrum of machine learning domains, with respect to the important

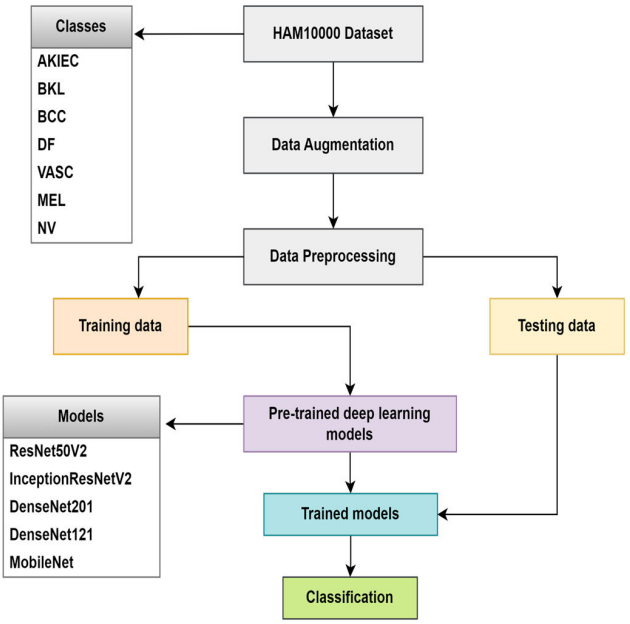

FIGURE 5. Flow diagram of implementation of pre-trained models.

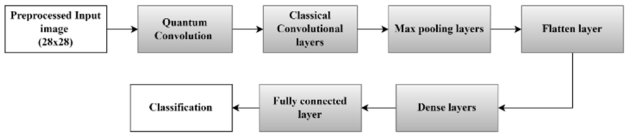

FIGURE 6. Quanvolutional neural network model.

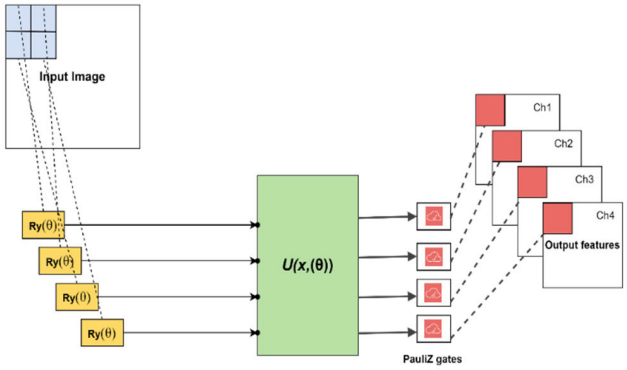

FIGURE 7. Quantum convolutional process with RY rotations and PauliZ gates.

feature of image recognition. Their prowess largely hinges on their knack for systematically discerning and extracting intricate features from datasets. The extraction of these features relies on various layers of transformations, with particular emphasis on the convolutional layer, which the model exhibits its name. In this work, the major contribution is based on a new transformation layer which is termed based on the quanvolutional layer or quantum convolution. Fig. 6 show the proposed Quanvolutional neural network model. Quanvolutional layers mainly works which is respect to the input data which are taken transformed locally by using multiple random quantum circuits which are involved for the transformations considering various on the basis of work on input data by locally transforming it using multiple random quantum circuits. As involved quantum transforms yield meaningful outcomes for classification, this algorithm could be valuable for quantum computers, as it necessitates small quantum circuits with minimal or there are corrections of errors in the process. The major difference between quantum circuits and classical convolutions are based on the potential complexity of the kernels they produce. Quantum circuits can generate immensely complex kernels, the computation of which may be prohibitively challenging for classical methods, at least theoretically. PennyLane is used to implement this procedure, which is basically software framework with open source which are involved for various needs of quantum machine learning algorithms, quantum chemistry and also involves quantum computing which can run on any hardware [43].

Fig. 7 exhibits Quantum convolutional process with RY rotations and PauliZ gates. Table 2 indicates types of Qubit rotation used in this study and Table 3 listout types of gates used in this study. Steps involved in quantum convolutional layer:

TABLE 2. Types of qubit rotation used in this study.

Function	Description
RX(phi, wires[, id])	The single qubit X rotation
RY(phi, wires[, id])	The single qubit Y rotation
RZ(phi, wires[, id])	The single qubit Z rotation

TABLE 3. Types of gates used in this study.

PennyLane Class name	Description	Mathematical representation
PauliX(*params [, wires, id])	The Pauli X gate is analogous to the classical NOT gate. It flips the state of a qubit, effectively changing a qubit in the $\|0\rangle$ state to the $\|1\rangle$ state and vice versa.	X = |0 1| |1 0|
PauliY(*params [, wires, id])	The Pauli Y gate is like the Pauli X gate but with a phase change. It performs a bit-flip operation along with a phase change. It is akin to a classical NOT gate followed by a bit-flip.	Y = |0 -i| |-i 0|
PauliZ(*params [, wires, id])	The Pauli Z gate leaves the $\|0\rangle$ state unchanged but changes the sign of the $\|1\rangle$ state. It is akin to a classical NOT gate but without changing the state, only the phase.	Z = |1 0| |0 -1|

TABLE 4. Sequential classical layers of proposed model.

Layer	Output shape	Parameters
Convolution2D-1	12x12x32	1184
Convolution2D-2	10x10x64	18496
Convolution2D-3	8x8x128	73856
Convolution2D-4	6x6x256	295168
max_pooling2d-1	3x3x256	0
max_pooling2d-2	1x1x256	0
Flatten	256	0
Dense-1	128	32896
Dense-2	64	8256
Dense-3	7	455

- Initially, we resize the images to 28×28. A small portion of the input image, specifically a 2×2 region, is encoded into a quantum circuit.
- A PennyLane "default. Qubit" [43] device was initialized to simulate a four-qubit system. In this study, this is accomplished by applying parameterized rotations of RX, RY, and RZ with angles scaled by a factor of pi, to the qubits initialized based on the ground state, along with a single layer of random circuitry.
- A quantum computation involving a unitary operation U is executed on the system. This unitary operation can be generated based on various quantum circuits.
- Finally, the developed quantum system is to be measured which is based on the results of various classical expectation values done in the process. In this process, it is directly utilized based on these raw expectation values. Here we have explored using Pauli-X, Pauli-Y, Pauli-Z gates, estimating 4 expectation values.

Each expectation value corresponds uniquely to a channel in a single output pixel, mirroring the structure of a standard convolutional layer. Repeating this method across multiple sections enables scanning of the entire input image, leading to the formation of an output object organized as a multi-channel image. Fig. 8 clearly shows resolution down sampling and some local distortion caused by the quantum kernel. Conversely, the overall shape of the image remains intact, consistent with the behavior expected of a convolutional layer. Subsequently, quantum convolution can be succeeded by additional quantum layers or classical layers. In this study, we added classical layers after the quantum convolutional layer along with SoftMax activation function at classification layer. Finally, the model consists of 430311 trainable parameters in total with 0 non-trainable parameters. The classical layers proposed in this study are given in Table 4.

G. QUANTUM SUPPORT VECTOR MACHINE (QSVM)

Support Vector Machines (SVMs) have earned widespread acclaim in the realm of machine learning due to their remarkable proficiency in tackling binary classification tasks.

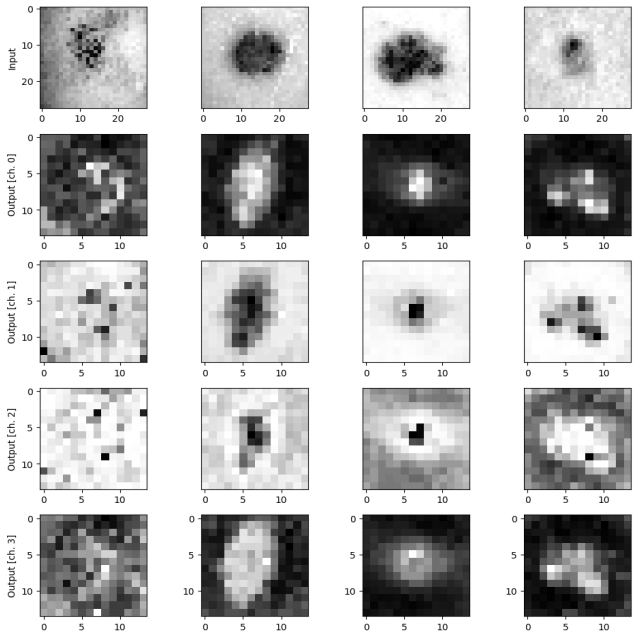

FIGURE 8. The four output channels generated by the quantum convolution after using RY rotations and PauliZ gates.

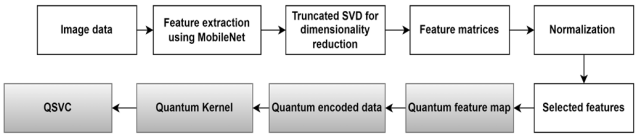

FIGURE 9. Proposed quantum support vector machine pipeline.

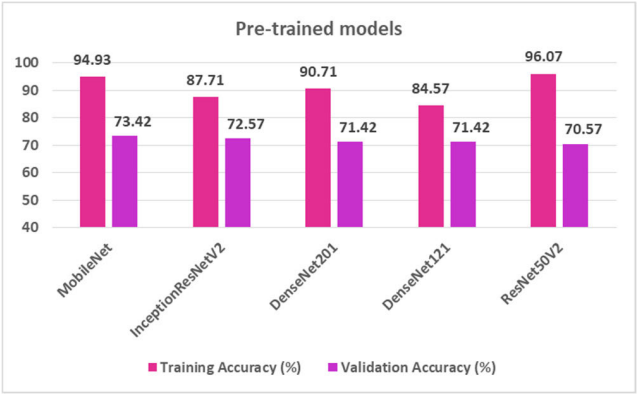

FIGURE 10. Results of selected pre-trained networks.

Notably, they excel at managing datasets with both linear and non-linear separability, as demonstrated by the influential work of Cortes and Vapnik. This versatility makes SVMs a popular choice across various domains, from finance to healthcare and beyond [44]. In SVMs, a decision boundary, termed the hyperplane, is utilized to discern between two classes within a dataset. This hyperplane is established based on a collection of data points referred to as support vectors. Quantum Support vector classifier (QSVC) is

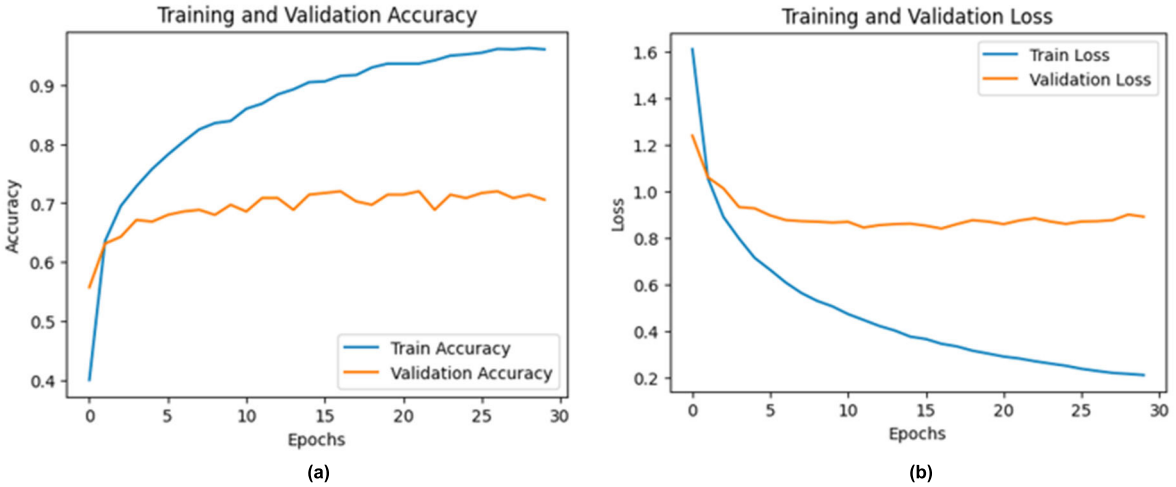

FIGURE 11. Comparison plots of (a) Epochs vs Accuracy plot, (b) Epochs vs Loss plot of ResNet50V2.

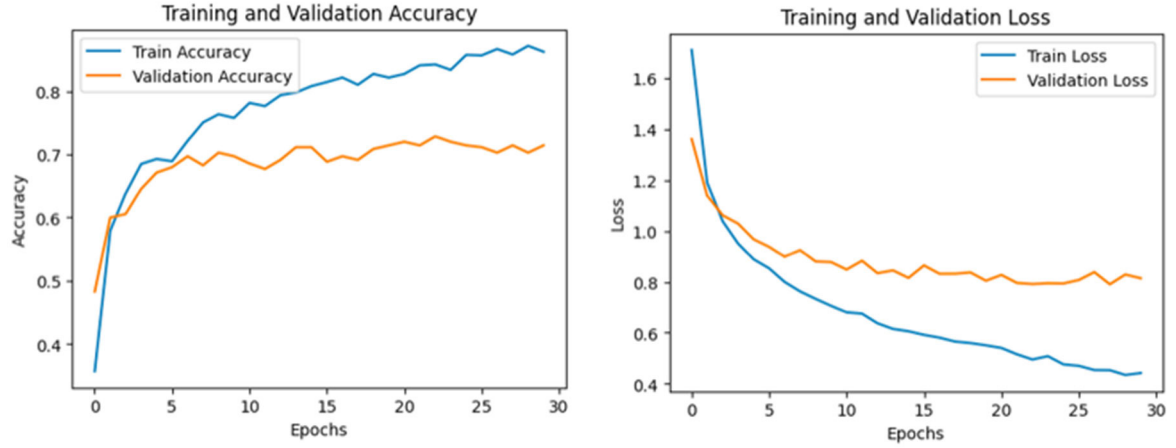

FIGURE 12. Comparison plots of (a) Epochs vs Accuracy Plot, (b) Epochs vs Loss Plot of InceptionResNetV2.

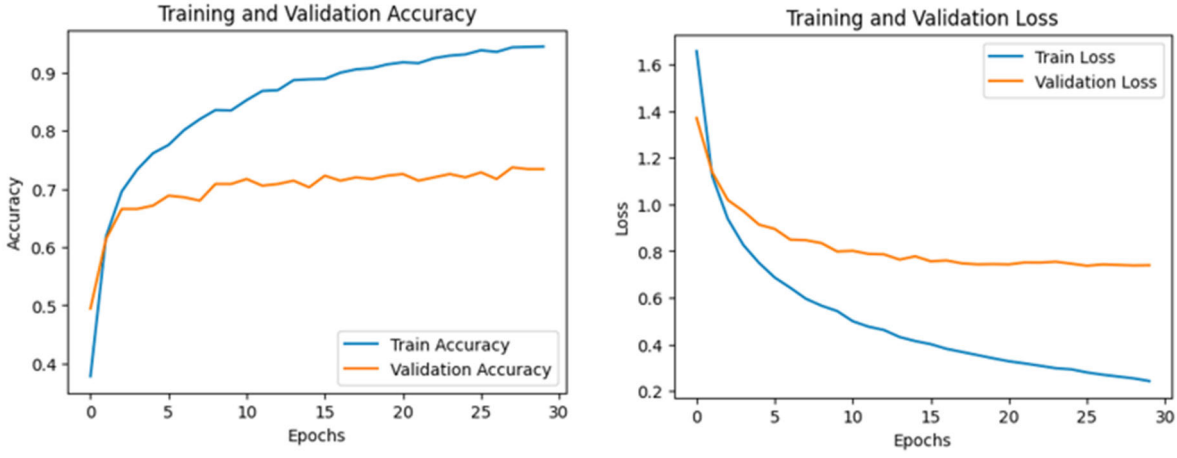

FIGURE 13. Comparison plots of (a) Epochs vs Accuracy Plot, (b) Epochs vs Loss Plot of MobileNet.

a quantum machine learning method available through the Qiskit library, which provides a way for multi-classification. Utilizing quantum circuits, the QSVC algorithm enhances classical SVMs by transforming input data into quantum states and exploiting quantum interference and entanglement. This involves the process of uncovering various optimal

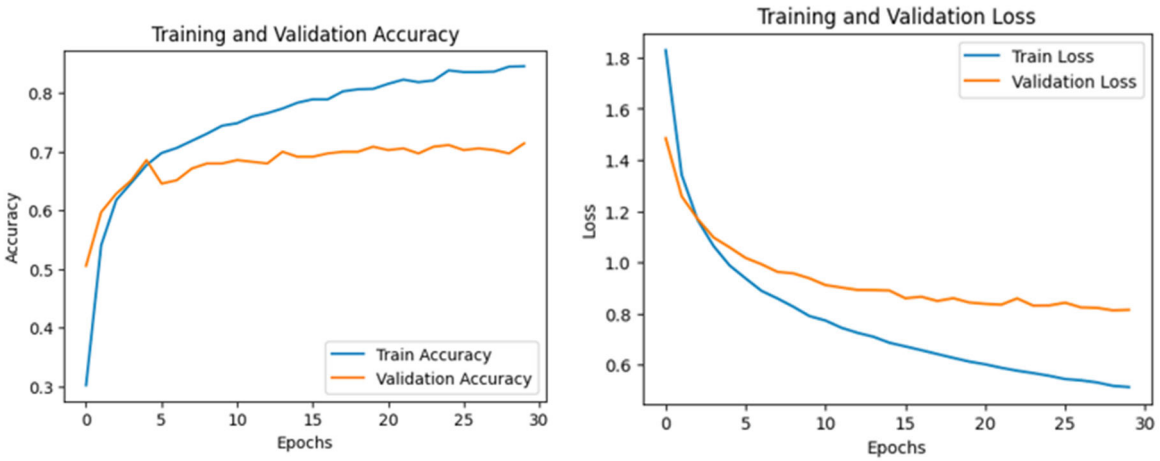

FIGURE 14. Comparison plots of (a) Epochs vs Accuracy Plot, (b) Epochs vs Loss Plot of DenseNet121.

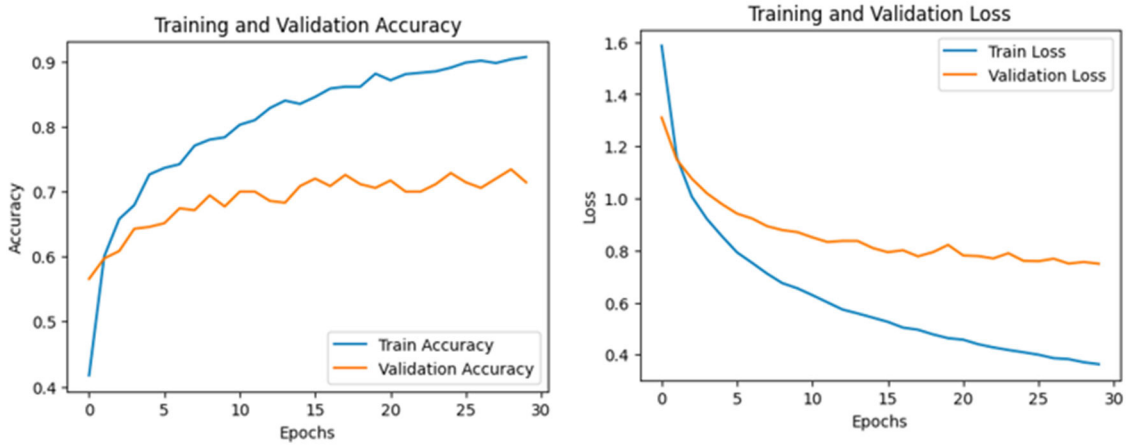

FIGURE 15. Comparison plots of (a) Epochs vs Accuracy Plot, (b) Epochs vs Loss Plot of DenseNet201.

hyperplane which are effectively separates data points to the exclusively classes which involves how it maximizes the margin involvement between the methods. QSVC, integrating quantum technology, offers potential for augmenting classification performance in contrast to standard SVM algorithms [24].

Feature extraction using Resnet50 pre-trained network is used to extract features from ECG images to implement Pegasus Quantum SVC [23]. Fig. 9 shows the proposed Quantum support vector machine pipeline. In this study, feature extraction using MobileNet pre-trained network is implemented. Features were extracted from the final max pooling layer. Truncated Singular Value Decomposition (SVD) serves as a matrix factorization technique employed in machine learning for linear dimensionality reduction. However, truncated SVD does not require the feature matrix, X to be centered. Truncated SVD accepts sparse matrices. Subsequently, min-max normalization is employed to conduct a linear transformation on the feature matrices. This technique gets all the scaled data in the range (0, 1). The selected features were then converted to quantum data using ZZ.

Feature Map, a quantum machine learning (QML) encoding method is utilized, which maps classical data to quantum state amplitudes. Its purpose is to identify pairwise correlations among input features and leverage them for classification tasks. Initiating the process is Quantum State Initialization, paving the way for Feature Encoding. Here, the Hadamard gate is employed to create a superposition of $|0\rangle$ and $|1\rangle$. Subsequently, ZZ Gate Implementation ensues, with the ZZ gate being applied between qubits 0 and 1 [23]. A kernel can generate the scalar products based on the feature map employed, which makes the optimization process more efficient and less computationally intensive. Here, FidelityQuantumKernel from Qiskit library is used. Then these kernels are passed to the QSVC function for multi-classification.

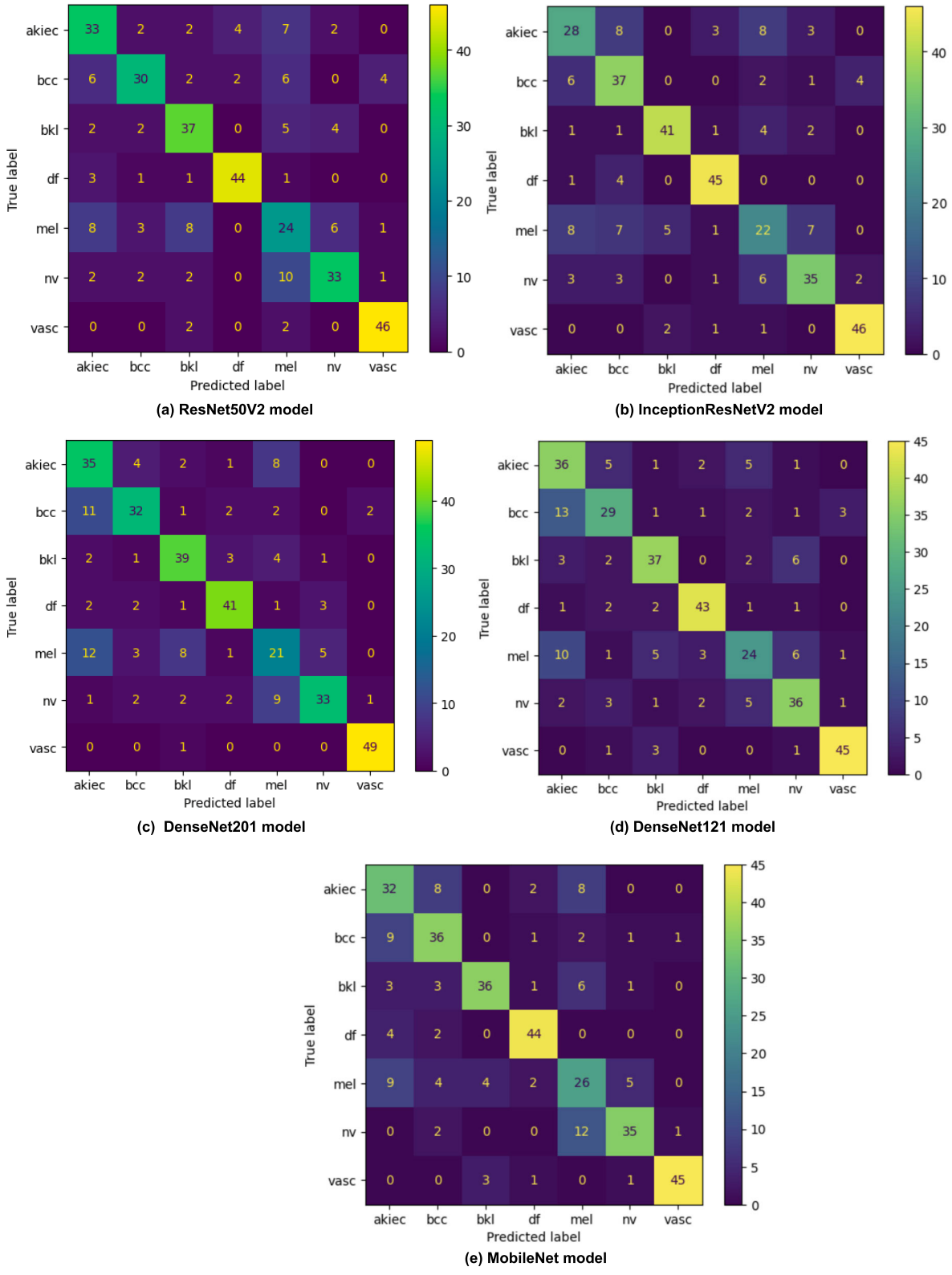

FIGURE 16. (a) – (e) Confusion matrix of pre-trained models.

IV. RESULTS AND DISCUSSION

In this section, we delve into the results obtained from the experimentation involving pre-trained neural network models, Quanvolutional neural network, and the quantum support vector classifier. Additionally, a comparison of results produced using combination of three qubit

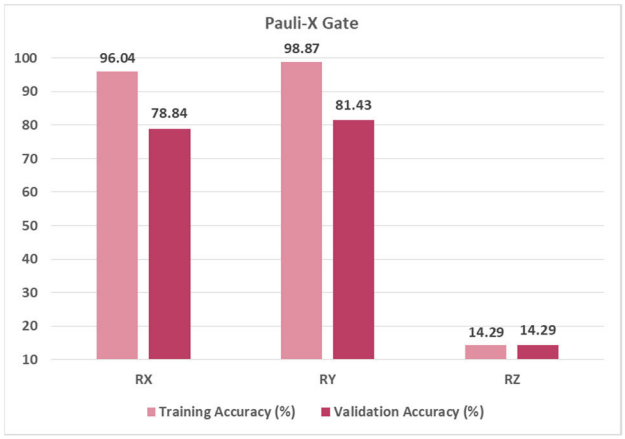

FIGURE 17. Model results with RX. RY and RZ Qubit rotation with Pauli-X gate in quantum convolution.

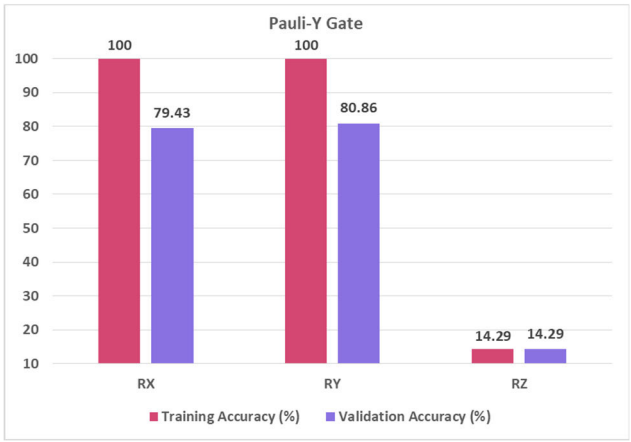

FIGURE 18. Model results with RX, RY and RZ Qubit rotation with Pauli-Y gate in quantum convolution.

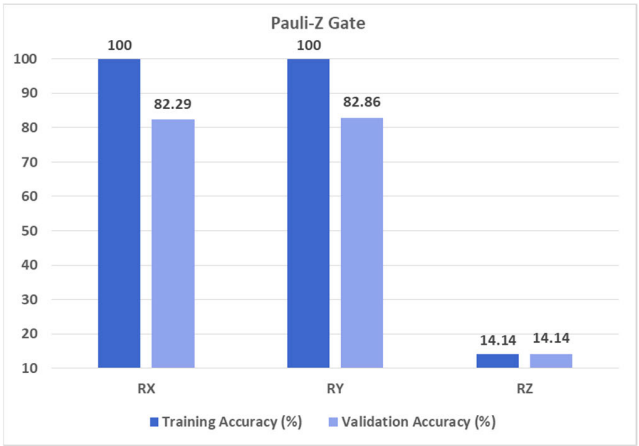

FIGURE 19. Model results with RX, RY and RZ Qubit rotation with Pauli-Z gate in quantum convolution.

rotations and Pauli gates in Quanvolutional neural network is discussed.

TABLE 5. Performance metrics of Quanvolutional neural network with (Ry rotation and Pauli Z gate).

Different Class	*Precision*	*Recall*	*F1-score*	*Support*
akiec	0.83	0.86	0.84	50
bcc	0.90	0.92	0.91	50
bkl	0.79	0.82	0.80	50
df	0.90	0.88	0.89	50
mel	0.74	0.70	0.72	50
nv	0.71	0.74	0.73	50
vasc	0.94	0.88	0.91	50

TABLE 6. Performance metrics of QSVC.

Class	*Precision*	*Recall*	*F1-score*	*Support*
akiec	0.72	0.78	0.75	50
bcc	0.73	0.80	0.76	50
bkl	0.65	0.86	0.74	50
df	0.80	0.90	0.85	50
mel	0.71	0.58	0.64	50
nv	0.67	0.48	0.56	50
vasc	0.88	0.74	0.80	50

The preprocessed data under seven classes were fed into five pre-trained neural network models such as MobileNet, InceptionResNetV2, DenseNet201, DenseNet121 and ResNet50V2, by resizing the data with respect to the models input size. MobileNet produced the highest classification accuracy of 73.42% among other pre-trained networks as shown in Fig. 10. The Fig. 11 shows that ResNet50V2 produced the least accuracy compared to other models with maximum loss during validation. InceptionResNetV2 produced the second highest accuracy among other pre-trained networks with minimal loss. The Fig. 12 and Fig. 13 shows the comparison between training and validation loss of InceptionResNet50V2 and MobileNet models. DenseNet201 and DenseNet121 produced the same classification accuracy of 71.42%, but in the Fig. 14 and Fig. 15, it indicates that training and validation loss of DenseNet121 is less compared to DenseNet201. From the observation of confusion matrix of pre-trained models shown in Fig. 16(a) to Fig. 16(e), pre-trained models performed a promising classification task on "df" and "vasc" classes, in contrast to "mel" and "nv" classes. Other classes such as "akiec", "bcc" and "bkl" are moderately classified.

Images are resized to 28 × 28 pixels and normalized before passing it through the quantum convolutional layer. Images are resized to such small resolution to overcome the computational limitation in this study. Furthermore, classification accuracies of combination of different qubit

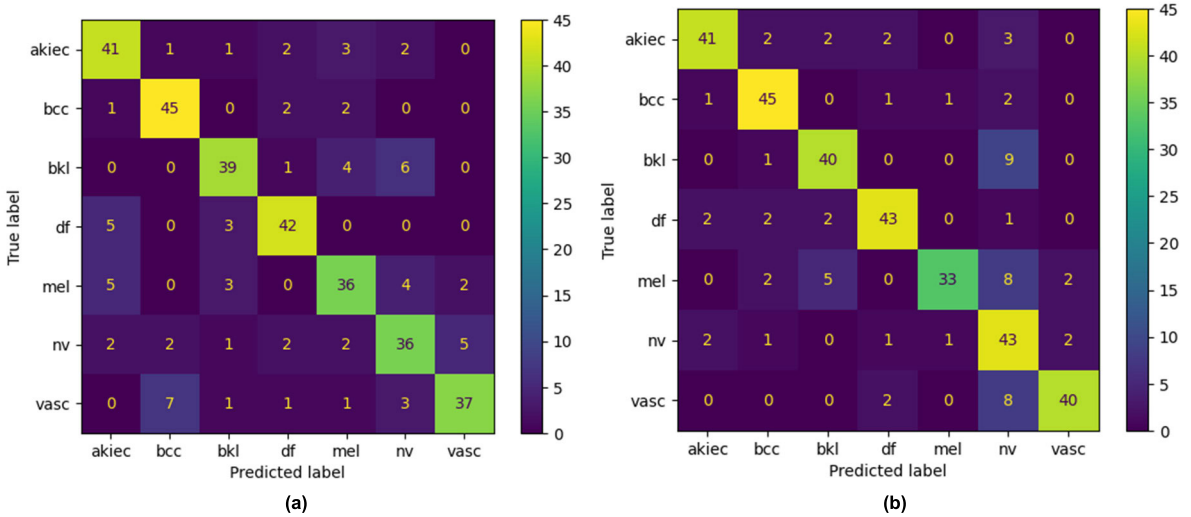

FIGURE 20. Confusion matrix of (a) RX, and (b) RY Qubit rotation with Pauli-X gate.

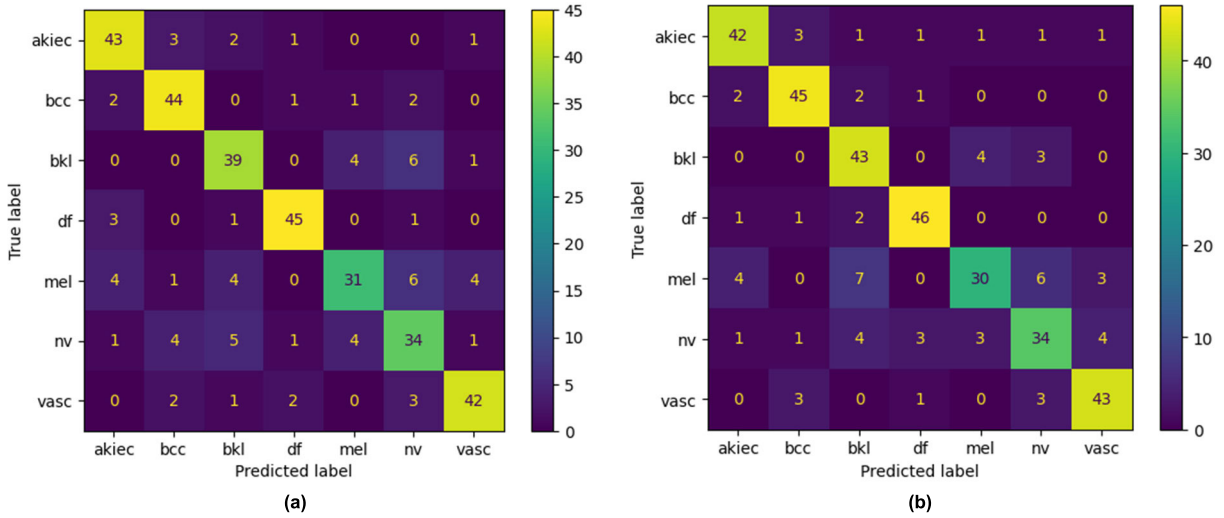

FIGURE 21. Confusion matrix of (a) RX, and (b) RY Qubit rotation with Pauli-Y gate.

rotation encoding and Pauli gate measurements are discussed. By observing Fig. 17 and Fig. 18, the Rx rotation encoding produced the validation accuracy around 79% in Pauli X and Pauli Y gate measurements as shown. The Ry the rotation encoding produced the validation accuracy of 81.43% and 80.86% in Pauli X and Pauli Y gates respectively. From the Fig. 19, we can observe that the combination of Ry rotation encoding along with Pauli Z gate measurement at decoding in quantum convolutional layer produced the highest classification accuracy of 82.86%.

Similarly, the combination of Rx rotation encoding along with Pauli Z gate measurement at decoding in quantum convolutional layer produced the second highest classification accuracy of 82.29%. The least classification accuracy is produced by Rz rotation encoding in all three Pauli gates. Thus, Rx qubit rotation encoding is not suitable for skin disease classification. From the observation of confusion matrix of Quanvolutional neural network models shown in Fig. 20, Fig. 21 and Fig. 22, classes such as ''mel'' and ''nv'' instances are less classified than other classes.

The Table 5 conveys that 'akiec' and 'bcc' stand out with precision, recall, and F1-scores all above 0.8, indicating robust performance. 'bkl' and 'df' also demonstrate strong precision and recall above 0.7, with F1-scores around 0.8 and 0.9 respectively. 'mel' and 'nv' show slightly lower but still acceptable precision, recall, and F1-scores around 0.7. 'vasc' exhibits exceptional precision of 0.94 and recall of 0.88, resulting in an impressive F1-score of 0.91. Overall, the model showcases varying degrees of effectiveness across different classes, with some achieving notably strong predictive capabilities. Thus, by increasing the input image size during Quanvolutional neural network model creation, one

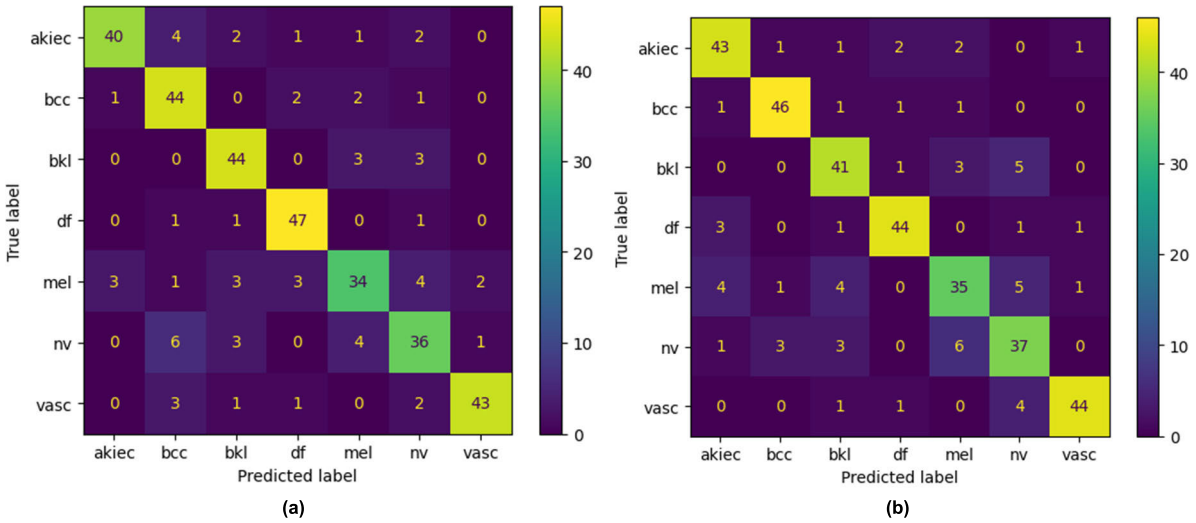

FIGURE 22. Confusion matrix of (a) RX, and (b) RY Qubit rotation with Pauli-Z gate.

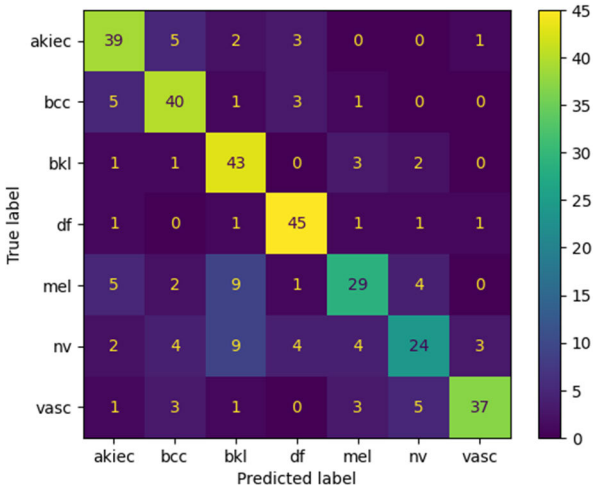

FIGURE 23. Confusion matrix of QSVC.

can reduce the loss in image resolution and achieve improved results in future. In this proposed study, due to computing limitations, a reduced dimension of 28 × 28 pixel images is used. From the results of pre-trained models, MobileNet is selected to extract features for building QSVC model, since it produced the highest classification accuracy among other models. Qiskit library is used to perform QSVC in this study. QSVC produced the classification accuracy of 72.5%. By observing Fig. 23, we understand that ''mel'' and ''nv'' classes are poorly classified which leads to less classification accuracy of the QSVC model.

The Table 6 shows the specificity for class 'akiec' was 0.72, indicating that 72% of the models predicted as 'akiec' were classified correctly, while recall was 0.78, indicating that actual 'akiec' models were identified 78% correctly F1-score of 'akiec' is 0.75, representing a balanced measure of precision and recall. Similarly, the precision, recall, and F1-score are 0.73, 0.80, and 0.76 for the 'bcc' class, respectively. The 'bkl' class exhibits a low precision of 0.65 but a high recall of 0.86, resulting in an F1-score of 0.74.

In contrast, the 'df' class exhibits good precision (0.80), recall (0.90), and F1-score (0.85), indicating a robust performance. Finally, the 'vasc' class achieves the highest precision (0.88) and recall (0.74), resulting in an F1-score of 0.80. However, 'mel' and 'nv' classes show low recall values of 0.58 and 0.48 respectively, indicating some difficulty in correctly identifying instances of these classes. In addition, by observing the confusion matrix of all the proposed models in this study, ''mel'' and ''nv'' classes are less classified than other classes. It can be because of the similarity in the appearance of Melanocytic nevi (nv) and Melanoma (mel). This shows the importance of skin lesion disease classification because Nevis are non-cancerous, while Melanoma is cancerous.

V. CONCLUSION

This study aimed to assess the effectiveness of quantum machine learning concepts and models in classifying skin diseases. The study showcased the superiority of QML models over classical counterparts. The novel quanvolutional neural network models developed in this research exhibited outstanding performance, achieving a classification accuracy of 82.86%, surpassing previously trained models. The quantum support vector classifier demonstrated comparable performance to the previously trained models. Only a few concepts of quantum computing were explored in this study. Exploring the theories of quantum computing and applying its potential to machine learning holds great promise. Furthermore, the incorporation of quantum computing principles into machine learning algorithms has the potential to solve the complex challenges that traditional computing

methods try to overcome and indeed, the future of this area looks to be it is a great hope. Quantum Machine Learning (QML) models have tremendous potential for breakthroughs by integrating quantum hardware, enhancing existing medical systems and diagnostic capabilities This integration holds promise to improve diagnostic accuracy and improved performance.

REFERENCES

[1] R. R. Yotsu, L. C. Fuller, M. E. Murdoch, W. H. van Brakel, C. Revankar, M. Y. T. Barogui, J. A. R. Postigo, D. A. Dagne, K. Asiedu, and R. J. Hay, "A global call for action to tackle skin-related neglected tropical diseases (skin NTDs) through integration: An ambitious step change," *PLOS Neglected Tropical Diseases*, vol. 17, no. 6, Jun. 2023, Art. no. e0011357, doi: 10.1371/journal.pntd.0011357.

[2] K. Urban, S. Chu, C. Scheufele, R. L. Giesey, S. Mehrmal, P. Uppal, and G. R. Delost, "The global, regional, and national burden of fungal skin diseases in 195 countries and territories: A cross-sectional analysis from the global burden of disease study 2017," *JAAD Int.*, vol. 2, pp. 22–27, Mar. 2021, doi: 10.1016/j.jdin.2020.10.003.

[3] A. Kavita, J. S. Thakur, and T. Narang, "The burden of skin diseases in India: Global burden of disease study 2017," *Indian J. Dermatol., Venereol. Leprol.*, vol. 89, pp. 421–425, Oct. 2021, doi: 10.25259/ijdvl_978_20.

[4] K. K. Brar and O. J. Shiney, "Computer-aided diagnosis and analysis of skin cancer from dermoscopic images in India," *Current Med. Imag. Formerly Current Med. Imag. Rev.*, vol. 20, pp. 1–14, Aug. 2023, doi: 10.2174/1573405620666230410092618.

[5] H. Sung, J. Ferlay, R. L. Siegel, M. Laversanne, I. Soerjomataram, A. Jemal, and F. Bray, "Global cancer statistics 2020: GLOBOCAN estimates of incidence and mortality worldwide for 36 cancers in 185 countries," *CA, Cancer J. Clinicians*, vol. 71, no. 3, pp. 209–249, May 2021, doi: 10.3322/caac.21660.

[6] T. Ramamoorthy, S. Leburu, V. Kulothungan, and P. Mathur, "Regional estimates of noncommunicable diseases associated risk factors among adults in India: Results from national noncommunicable disease monitoring survey," *BMC Public Health*, vol. 22, no. 1, pp. 1–13, Dec. 2022, doi: 10.1186/s12889-022-13466-5.

[7] M. Ahammed, M. A. Mamun, and M. S. Uddin, "A machine learning approach for skin disease detection and classification using image segmentation," *Healthcare Anal.*, vol. 2, Nov. 2022, Art. no. 100122, doi: 10.1016/j.health.2022.100122.

[8] M. Jagdish, S. P. G. Guamangate, M. A. G. López, J. A. De La Cruz-Vargas, and M. E. R. Camacho, "Advance study of skin diseases detection using image processing methods," *Nat. Volatiles Essent. Oils*, vol. 9, no. 1, pp. 997–1007, 2022.

[9] F. Bozkurt, "Skin lesion classification on dermatoscopic images using effective data augmentation and pre-trained deep learning approach," *Multimedia Tools Appl.*, vol. 82, no. 12, pp. 18985–19003, May 2023, doi: 10.1007/s11042-022-14095-1.

[10] H. Younis, M. H. Bhatti, and M. Azeem, "Classification of skin cancer dermoscopy images using transfer learning," in *Proc. 15th Int. Conf. Emerg. Technol. (ICET)*, Dec. 2019, pp. 1–4, doi: 10.1109/ICET48972.2019.8994508.

[11] V. Anand, S. Gupta, S. R. Nayak, D. Koundal, D. Prakash, and K. D. Verma, "An automated deep learning models for classification of skin disease using dermoscopy images: A comprehensive study," *Multimedia Tools Appl.*, vol. 81, no. 26, pp. 37379–37401, Nov. 2022, doi: 10.1007/s11042-021-11628-y.

[12] P. Anil, B. J. L. Narayana, G. K. T. Reddy, S. R. Choudhary, and K. S. Sri, "Skin cancer classification with DenseNet deep convolutional neural network," in *Proc. 4th IEEE Global Conf. Adv. Technol. (GCAT)*, Oct. 2023, pp. 1–6, doi: 10.1109/gcat59970.2023.10353529.

[13] K. Thurnhofer-Hemsi and E. Domínguez, "A convolutional neural network framework for accurate skin cancer detection," *Neural Process. Lett.*, vol. 53, no. 5, pp. 3073–3093, Oct. 2021, doi: 10.1007/s11063-020-10364-y.

[14] A. Panthakkan, S. M. Anzar, S. Jamal, and W. Mansoor, "Concatenated xception-ResNet50—A novel hybrid approach for accurate skin cancer prediction," *Comput. Biol. Med.*, vol. 150, Nov. 2022, Art. no. 106170, doi: 10.1016/j.compbiomed.2022.106170.

[15] R. Hassan Bedeir, R. Orban Mahmoud, and H. H. Zayed, "Automated multi-class skin cancer classification through concatenated deep learning models," *IAES Int. J. Artif. Intell.*, vol. 11, no. 2, p. 764, Jun. 2022, doi: 10.11591/ijai.v11.i2.pp764-772.

[16] J. Shalf, "The future of computing beyond Moore's law," *Phil. Trans. Roy. Soc. A, Math., Phys. Eng. Sci.*, vol. 378, no. 2166, Mar. 2020, Art. no. 20190061, doi: 10.1098/rsta.2019.0061.

[17] Y. Ding and A. Javadi-Abhari, "Quantum and post-Moore's law computing," *IEEE Internet Comput.*, vol. 26, no. 1, pp. 5–6, Jan. 2022, doi: 10.1109/MIC.2021.3133675.

[18] A. Abbas, D. Sutter, C. Zoufal, A. Lucchi, A. Figalli, and S. Woerner, "The power of quantum neural networks," *Nature Comput. Sci.*, vol. 1, no. 6, pp. 403–409, Jun. 2021, doi: 10.1038/s43588-021-00084-1.

[19] L. Wei, H. Liu, J. Xu, L. Shi, Z. Shan, B. Zhao, and Y. Gao, "Quantum machine learning in medical image analysis: A survey," *Neurocomputing*, vol. 525, pp. 42–53, Mar. 2023, doi: 10.1016/j.neucom.2023.01.049.

[20] S. Otgonbaatar, G. Schwarz, M. Datcu, and D. Kranzlmüller, "Quantum transfer learning for real-world, small, and high-dimensional remotely sensed datasets," *IEEE J. Sel. Topics Appl. Earth Observ. Remote Sens.*, vol. 16, pp. 9223–9230, 2023, doi: 10.1109/JSTARS.2023.3316306.

[21] T. Hur, L. Kim, and D. K. Park, "Quantum convolutional neural network for classical data classification," *Quantum Mach. Intell.*, vol. 4, no. 1, p. 3, Jun. 2022, doi: 10.1007/s42484-021-00061-x.

[22] A. Sebastianelli, D. A. Zaidenberg, D. Spiller, B. Le Saux, and S. Ullo, "On circuit-based hybrid quantum neural networks for remote sensing imagery classification," *IEEE J. Sel. Topics Appl. Earth Observ. Remote Sens.*, vol. 15, pp. 565–580, 2022, doi: 10.1109/JSTARS.2021.3134785.

[23] S. Prabhu, S. Gupta, G. M. Prabhu, A. V. Dhanuka, and K. V. Bhat, "QuCardio: Application of quantum machine learning for detection of cardiovascular diseases," *IEEE Access*, vol. 11, pp. 136122–136135, 2023, doi: 10.1109/ACCESS.2023.3338145.

[24] J. K. A. Das and M. Malhotra, "Quantum machine learning: An effective approach to high-dimensional learning," in *Proc. 6th Int. Conf. Comput. Syst. Inf. Technol. Sustain. Solutions (CSITSS)*, Dec. 2022, pp. 1–6, doi: 10.1109/CSITSS57437.2022.10026399.

[25] N. Abdullayev, L. Aliyeva, and J. Hasanov, "Comparative study of quantum to classical machine learning algorithms for breast cancer classification," in *Proc. IEEE 17th Int. Conf. Appl. Inf. Commun. Technol. (AICT)*, Oct. 2023, pp. 1–6, doi: 10.1109/aict59525.2023.10313161.

[26] M. Munshi, R. Gupta, N. K. Jadav, Z. Polkowski, S. Tanwar, F. Alqahtani, and W. Said, "Quantum machine learning-based framework to detect heart failures in healthcare 4.0," *Softw., Pract. Exp.*, vol. 54, no. 2, pp. 168–185, Feb. 2024, doi: 10.1002/spe.3264.

[27] G. Abdulsalam, S. Meshoul, and H. Shaiba, "Explainable heart disease prediction using ensemble-quantum machine learning approach," *Intell. Autom. Soft Comput.*, vol. 36, no. 1, pp. 761–779, 2023, doi: 10.32604/iasc.2023.032262.

[28] R. Das, "Quantum machine learning based computer aided diagnosis for skin cancer detection: A statistical performance analysis over classical approach," in *Proc. Int. Conf. Trends Quantum Comput. Emerg. Bus. Technol. (TQCEBT)*, Oct. 2022, pp. 1–5, doi: 10.1109/TQCEBT54229.2022.10041478.

[29] P. Tschandl, C. Rosendahl, and H. Kittler, "The HAM10000 dataset, a large collection of multi-source dermatoscopic images of common pigmented skin lesions," *Sci. Data*, vol. 5, no. 1, pp. 1–9, Aug. 2018, doi: 10.1038/sdata.2018.161.

[30] C. Shorten and T. M. Khoshgoftaar, "A survey on image data augmentation for deep learning," *J. Big Data*, vol. 6, no. 1, pp. 1–48, Dec. 2019, doi: 10.1186/s40537-019-0197-0.

[31] M. R. Roh, P. Eliades, S. Gupta, and H. Tsao, "Genetics of melanocytic nevi," *Pigment Cell Melanoma Res.*, vol. 28, no. 6, pp. 661–672, Nov. 2015, doi: 10.1111/pcmr.12412.

[32] K. Saginala, A. Barsouk, J. S. Aluru, P. Rawla, and A. Barsouk, "Epidemiology of melanoma," *Med. Sci.*, vol. 9, no. 4, p. 63, Oct. 2021, doi: 10.3390/medsci9040063.

[33] N. Girdhar, A. Sinha, and S. Gupta, "DenseNet-II: An improved deep convolutional neural network for melanoma cancer detection," *Soft Comput.*, vol. 27, no. 18, pp. 13285–13304, Sep. 2023, doi: 10.1007/s00500-022-07406-z.

[34] E. Dika, F. Scarfì, M. Ferracin, E. Broseghini, E. Marcelli, B. Bortolani, E. Campione, M. Riefolo, C. Ricci, and M. Lambertini, "Basal cell carcinoma: A comprehensive review," *Int. J. Mol. Sci.*, vol. 21, no. 15, p. 5572, Aug. 2020, doi: 10.3390/ijms21155572.

[35] V. Palaniappan and K. Karthikeyan, "Bowen's disease," *Indian Dermatol. Online J.*, vol. 13, no. 2, p. 177, 2022, doi: 10.4103/idoj.idoj_257_21.
[36] J. D. Bouaziz, T. A. Duong, M. Jachiet, C. Velter, P. Lestang, C. Cassius, A. Arsouze, E. Domergue Than Trong, M. Bagot, E. Begon, L. Sulimovic, and M. Rybojad, "Vascular skin symptoms in COVID-19: A French observational study," *J. Eur. Acad. Dermatol. Venereol.*, vol. 34, no. 9, pp. e451–e452, Sep. 2020, doi: 10.1111/jdv.16544.
[37] T. Mentzel, T. Wiesner, L. Cerroni, M. Hantschke, H. Kutzner, A. Rütten, M. Häberle, M. Bisceglia, F. Chibon, and J.-M. Coindre, "Malignant dermatofibroma: Clinicopathological, immunohistochemical, and molecular analysis of seven cases," *Modern Pathol.*, vol. 26, no. 2, pp. 256–267, Feb. 2013, doi: 10.1038/modpathol.2012.157.
[38] J. Gu, Z. Wang, J. Kuen, L. Ma, A. Shahroudy, B. Shuai, T. Liu, X. Wang, G. Wang, J. Cai, and T. Chen, "Recent advances in convolutional neural networks," *Pattern Recognit.*, vol. 77, pp. 354–377, May 2018, doi: 10.1016/j.patcog.2017.10.013.
[39] K. He, X. Zhang, S. Ren, and J. Sun, "Deep residual learning for image recognition," in *Proc. IEEE Conf. Comput. Vis. Pattern Recognit. (CVPR)*, Jun. 2016, pp. 770–778, doi: 10.1109/CVPR.2016.90.
[40] C. Szegedy, S. Ioffe, V. Vanhoucke, and A. A. Alemi, "Inception-v4, inception-ResNet and the impact of residual connections on learning," in *Proc. 31st AAAI Conf. Artif. Intell.*, 2017, pp. 4278–4284, doi: 10.1609/aaai.v31i1.11231.
[41] G. Huang, Z. Liu, L. Van Der Maaten, and K. Q. Weinberger, "Densely connected convolutional networks," in *Proc. IEEE Conf. Comput. Vis. Pattern Recognit. (CVPR)*, Jul. 2017, pp. 2261–2269, doi: 10.1109/CVPR.2017.243.
[42] A. G. Howard, M. Zhu, B. Chen, D. Kalenichenko, W. Wang, T. Weyand, M. Andreetto, and H. Adam, "MobileNets: Efficient convolutional neural networks for mobile vision applications," 2017, *arXiv:1704.04861*.
[43] M. Henderson, S. Shakya, S. Pradhan, and T. Cook, "Quanvolutional neural networks: Powering image recognition with quantum circuits," *Quantum Mach. Intell.*, vol. 2, no. 1, p. 2, Jun. 2020, doi: 10.1007/s42484-020-00012-y.
[44] C. Cortes and V. Vapnik, "Support-vector networks," *Mach. Learn.*, vol. 20, no. 3, pp. 273–297, 1995, doi: 10.1023/a:1022627411411.

S. SOFANA REKA is currently an Associate Professor with the School of Electronics Engineering, Vellore Institute of Technology, Chennai. She has published various international journals with high impact factor in her credit. Her research interests include smart grid, embedded systems, machine learning, the Internet of Things, and cyber physical systems. She is a reviewer of many SCI journals.

H. LEELA KARTHIKEYAN is currently pursuing the bachelor's degree with the School of Electronics Engineering, Vellore Institute of Technology, Chennai, specializing in electronics and computer engineering. His major research interests include artificial intelligence and machine learning.

A. JACK SHAKIL is currently pursuing the bachelor's degree with the School of Electronics Engineering, Vellore Institute of Technology, Chennai, specializing in electronics and computer engineering. His major research interests include data science and machine learning.

PRAKASH VENUGOPAL is currently an Associate Professor with the School of Electronics Engineering, Vellore Institute of Technology, Chennai. He has published many research papers in high-quality peer-reviewed journals and international conferences. His major research interests include embedded system design, real-time operating systems, battery management system in electric vehicle, smart grid, the Internet of Things, and machine learning.

MANIGANDAN MUNIRAJ received the B.E. degree in electronics and communication engineering from the University of Madras and the M.E. degree in mechatronics from Madras Institute of Technology, Anna University, Chennai, and the Ph.D. degree in underwater image processing from the Department of ECE, National Institute of Technology, Delhi, in February 2023. He was a Full Time Research Scholar in underwater image processing with the Department of ECE, National Institute of Technology. Before joining as an Assistant Professor with the SENSE School–VIT University, he had more than 13 years of work experience in various cross domain fields related to academic research, embedded industry, and intellectual property rights related to patents (drafting, filing, novelty search, and freedom to operate search). He has published papers in international journals and international conferences, and obtained various funding from AICTE (MODROBS) and DRDO Laboratory. His research interests include underwater image enhancement and restoration, atmospheric image dehazing, optical polarization imaging, embedded image processing, computer vision, digital signal processing, robotics, and the Internet of Things. He is a reviewer for SCI and IEEE journals.